CSIRO PUBLISHING

Aust. J. Chem. **2016**, *69*, 291–299
http://dx.doi.org/10.1071/CH15071

Full Paper

Aryl Naphthoates: A Conformational Analysis Supported by Single-Crystal X-Ray Diffraction

Jorge L. Jios,[A,E] *Rudolf Wartchow,*[B] *Gustavo A. Echeverría,*[C] *and Helmut Duddeck*[D]

[A]Unidad Plapimu-Laseisic (UNLP-CIC), Departamento de Química, Facultad de Ciencias Exactas, Universidad Nacional de La Plata, 47 esq. 115, (1900) La Plata, Argentina.
[B]Universität Hannover, Institut für Anorganische Chemie, Callinstr. 9, D-30167 Hannover, Germany.
[C]Departamento de Física, Facultad de Ciencias Exactas, Universidad Nacional de La Plata e IFLP (CONICET, CCT-La Plata), C. C. 67, 1900 La Plata, Argentina.
[D]Universität Hannover, Institut für Organische Chemie, Schneiderberg 1B, D-30167 Hannover, Germany.
[E]Corresponding author. Email: jljios@quimica.unlp.edu.ar

The conformational study by X-ray diffraction of 12 aroyl esters of *ortho*-acetyl phenols is reported. The data are supported by theoretical calculations and described in terms of co-planarity, intramolecular steric interference, and intermolecular contacts. The observed hindrance was correlated with the C=O stretching vibration values in infrared spectroscopy.

Manuscript received: 10 February 2015.
Manuscript accepted: 23 July 2015.
Published online: 27 August 2015.

Introduction

o-Acetylphenyl naphthoates are intermediates in the preparation of arylchromones, an important class of oxygen-containing heterocyclic compounds that are widespread in nature.[1] Structurally, these compounds are composed of two rigid aromatic rings connected by a relatively flexible ester fragment (–O–C(O)–). The *o*-acetyl pendant is also likely to move around the C(sp^2)–C(O) single bond. Looking at the whole molecule, the mobility on four chemical bonds is important to consider: (1) the aforementioned bond connecting the methyl carbonyl group with the phenyl ring; (2) the bond between the phenyl and the oxygen bridge C(sp^2)–O(sp^3); (3) the ester linkage C(O)–O, and (4) the bond between the carbonyl group and the naphthyl moiety (1-C10H7 or 2-C10H7). The conformation of esters of the type –C(O)–O–R (case 3) has been the subject of essential investigation since a very long time, revealing that the *Z* conformation is favoured over the *E* counterpart[2–6] (Chart 1). One of the reasons is the steric repulsion between the R groups in the *E* conformation. Also, the large rotational barrier about the C–O ester bond is attributed to resonance delocalization of the lone pair electrons of the ester oxygen.[5,6]

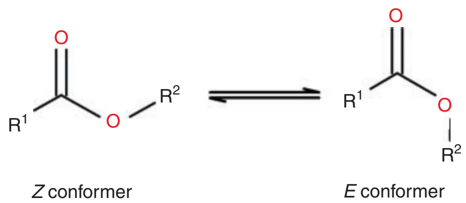

Chart 1. Conformations in the ester linkage.

In this paper, we report the X-ray structures and solid-state conformations of the acetylphenyl naphthoates **2**–**13** (Chart 2). The X-ray data of *o*-acetylphenyl 1-naphthoate (**1**)[7] was incorporated into this study for comparison. Apart from the structures reported in this study, no other X-ray diffraction data of acetylphenyl naphthoates was found. Therefore, only one X-ray-related structure, *o*-acetyl-4-methylphenyl 4-methylbenzoate, was reported in literature.[8] In order to clarify some questions about the structural properties and preferred conformations of the acetylphenyl naphthoate series, we have used *o*-acetylphenyl 1-naphthoate (**1**) and its constitutional isomer, *o*-acetylphenyl 2-naphthoate, as models, and used the density functional theory (DFT) for conformational searching and geometry optimization of the most stable conformers. The ^{1}H, ^{13}C, and ^{17}O NMR spectra were reported in our previous study.[9]

Results and Discussion

Theoretical Calculations

Due to the structural flexibility of the title molecules, the potential energy (E_p) curves around four torsion angles were obtained. Chart 2 shows the angles A–D and bonds investigated (in blue colour). The E_p curve of torsion A (C1–C1′ bond)

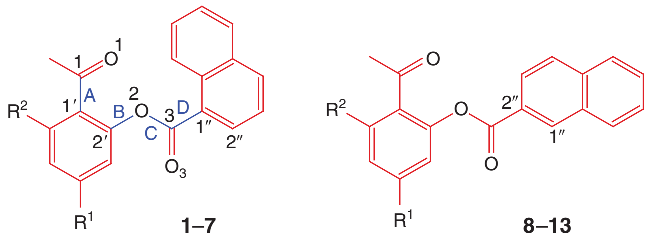

	R^1	R^3	Ar
1	H	H	1-naphthyl
2	NO_2	H	1-naphthyl
3	Br	H	1-naphthyl
4	Cl	H	1-naphthyl
5	F	H	1-naphthyl
6	CH_3	H	1-naphthyl
7	OCH_3	OCH_3	1-naphthyl
8	NO_2	H	2-naphthyl
9	Br	H	2-naphthyl
10	Cl	H	2-naphthyl
11	F	H	2-naphthyl
12	CH_3	H	2-naphthyl
13	OCH_3	OCH_3	2-naphthyl

Chart 2. Structures of the aryl naphthoates **1**–**13**.

delivered two conformers at 0° (s-*cis* configuration) and 180° (s-*trans* configuration), with the latter conformer being 1 kcal mol^{-1} more stable than the former conformer. Torsion B angle (C2′–O bond) shows two equivalent minima at ~ ±90°. Torsion C angle refers to the preferred conformation around the C(O)–O–R ester function. As described above, the *Z* conformation of esters is expected to be more stable than the *E* conformation[2–4] (Chart 1). In a previous work, phenyl esters of cinnamic acid showed that the *Z* conformation was 4.91 kcal mol^{-1} more stable than its *E* counterpart.[10] The E_p curve around torsion C angle shows only one minimum at 0° as the *E* conformer forces both aromatic rings to get close to each other (repulsive effect). The E_p difference between the two conformers, i.e. $E_p(E) - E_p(Z)$, is greater than 8 kcal mol^{-1}. Torsion D involves the rotation of naphthyl ring around the carbonyl group of the ester function. As expected, the isomer containing the 2-naphthyl ring shows a conjugative stabilization, with the s-*trans* (O3C3–C2″C1″ = 180°) being only 0.06 kcal mol^{-1} more stable than the s-*cis* conformer (0°). The molecule of **1** has a differential behaviour. The angle O3C3–C1″C2″ has two minima at −150° and 30°. The s-*trans* conformer is 1.05 kcal mol^{-1} more stable than the s-*cis* conformer. The conjugative stabilization is not enough to absorb the repulsive, very short interaction C=O3···H8″, and the carbonyl moiety deviates by ± 30° on the naphthyl ring plane.

After the conformational searching, the following energy minima were found for each of the four torsion angles investigated: 0° and 180° (A), 90° (B), 0° (C), and 30° and −150° for **1** and 0° and 180° for *o*-acetylphenyl 2-naphthoate (D). According to these results, four conformations were considered as starting points for further optimization at the B3LYP/6–311G(d,p) level of theory. This procedure was repeated for molecules **4** and **10** (with chlorine as an electron-accepting atom) and for **6** and **12** (with methyl as an electron-donating group). For better comparison between the results of the X-ray diffraction analysis and theoretical calculations, the energy of the conformation found in the crystal, with and without optimization, was also calculated at the same level of theory. The results are shown in Table 1.

Special attention was paid to the carbonyl group conformation. As stated before, when torsion angle A approaches 0° and 180°, the disposition of the carbonyl in the acetyl group is s-*cis* and s-*trans*, respectively. The carbonyl belonging to the ester is s-*trans* and s-*cis* when the torsion angle D is 0° and 180°, respectively. In all the molecules investigated, the most stable conformation for the acetyl and ester carbonyl is s-*trans* and s-*cis*, respectively. In the 1-naphthoyl series (compounds **1**, **4**, and **6**), the difference between the higher and lower potential energies, ΔE_p, of the conformation is up to 2.2 kcal mol^{-1}, whereas in the 2-naphthoyl series (*o*-acetylphenyl 2-naphthoate, **10** and **12**), ΔE_p is only 1.05 kcal mol^{-1}.

Looking at the results of population analysis, they show that the 1-naphthoyl series has 92–94 % of the population concentrated between the only two conformations with $\Delta E_p <$ 1 kcal mol^{-1}. For the 2-naphthoyl series, all the considered conformations (four of the four) are below 1 kcal mol^{-1}, and therefore each of them has a significant population distribution (above 8 %; see Table 1).

Considering the stability of different conformations in the gas phase, it is expected that in the crystal lattice, the molecule preferably acquires any of the conformations having $\Delta E_p <$ 1 kcal mol^{-1}. Because theoretical calculations do not take into account intermolecular interactions that may be involved in the crystal lattice, the differences between the conformations resulting in crystal formation, and the most stable, predicted by theoretical calculation, should be due to the effects of crystal packing.

Single-Crystal X-Ray Diffraction and Infrared Carbonyl Frequencies

Table 2 shows the crystal data of all new compounds investigated, whereas the selected interatomic distances, bond angles, and torsion angles are represented in Tables 3, 4, and 5, respectively. It is interesting to look at the co-planarity within the two parts of the molecules, the naphthoate and the acetylphenoxy residues, as well as the spatial orientation of both with respect to each other.

*1-Naphthoates **1–7***

Though substitution in the 4′- or in the 4′- and 6′-positions of the acetophenone ring does not significantly change any bond distances and bond angles (Tables 3 and 4), there are variations in the torsion angle (φ) behaviour, i.e. changes in the conformations (see Table 5). If the acetylphenoxy residues are monosubstituted (**2**–**6**), they display divergence from co-planarity between the aromatic ring and the acetyl carbonyl group. The absolute deviations for φ(O1–C1–C1′–C2′) are between 14° and 30°. Both orientations of C=O are represented, that towards the ester function or s-*cis* configuration (**1**, **5**–**7**) and that towards C6′ or s-*trans* configuration (**2**–**4**, Table 5). In the dimethoxy derivative **7**, however, the φ-value is slightly larger (33°), probably as a consequence of steric interference between the acetyl and the *ortho*-methoxy group.

The conformation of the ester group, linking the two aromatic systems, is *anti-periplanar* with torsion angles ψ(C2′–O2–C3–C1′) between 171° and 176°. These results are in agreement with the preferred *Z* conformation found in the ester group O3C3O2C2′[2–6] and also predicted by theoretical calculations (see above). However, there is a strong twist in the ester part with respect to the C–O single bond (Fig. 1). As can be observed in Table 5, this bend produces high distortion between aromatic rings (diedral angles between ring planes δ are between −42° and −81°). Theoretical calculations also predicted a minimum near 90° for the torsion angle connecting this C–O single bond

Table 1. Carbonyl configuration determined by theoretical calculations[A]
Values in brackets are torsion angles A and D (in degrees)

	1				*o*-Acetylphenyl 2-naphthoate			
	C=O				C=O			
Conformation	Acetyl	Ester	ΔE_p^C	Pop.[D]	Acetyl	Ester	ΔE_p^C	Pop.[D]
I	s-*Trans* (166.0)	s-*Cis* (166.2)	0.00	76.6	s-*Trans* (164.6)	s-*Cis* (174.0)	0.00	44.3
II	s-*Cis* (7.4)	s-*Cis* (−160.6)	0.92	15.8	s-*Cis* (−4.0)	s-*Cis* (−175.3)	0.97	8.4
III	s-*Trans* (166.3)	s-*Trans* (−20.7)	1.58	5.1	s-*Trans* (164.6)	s-*Trans* (−4.2)	0.06	40.0
IV	s-*Cis* (38.3)	s-*Trans* (30.5)	2.00	2.5	s-*Cis* (−4.2)	s-*Trans* (3.9)	1.05	7.3
Experimental[B]	s-*Cis* (−24.2)	s-*Cis* (165.1)	4.15	–	–	–	–	–
V[E]	s-*Cis* (7.5)	s-*Cis* (–60.6)	0.92	–	–	–	–	–
	4				**10**			
I	s-*Trans* (167.6)	s-*Cis* (166.3)	0.00	68.7	s-*Trans* (166.3)	s-*Cis* (173.9)	0.00	45.4
II	s-*Cis* (4.4)	s-*Cis* (−159.3)	0.90	25.1	s-*Cis* (−0.6)	s-*Cis* (−175.5)	0.96	8.2
III	s-*Trans* (168.8)	s-*Trans* (−20.9)	1.59	4.5	s-*Trans* (166.2)	s-*Trans* (−4.5)	0.09	38.9
IV	s-*Cis* (26.5)	s-*Trans* (29.2)	2.16	1.7	s-*Cis* (−3.6)	s-*Trans* (4.7)	1.05	7.5
Experimental[B]	s-*Trans* (−159.4)	s-*Cis* (−152.5)	4.47	–	s-*Cis* (3.3)	s-*Cis*(−171.2)	6.30	–
V[E]	s-*Trans* (−167.7)	s-*Cis* (−166.2)	0.00	–	s-*Cis*(-0.6)	s-*Cis* (−175.5)	0.96	–
	6				**12**			
I	s-*Trans* (168.8)	s-*Cis* (165.9)	0	74.9	s-*Trans* (167.3)	s-*Cis* (174.0)	0	44.3
II	s-*Cis* (3.4)	s-*Cis* (−161.5)	0.83	18.0	s-*Cis* (−3.6)	s-*Cis* (−175.1)	0.92	9.1
III	s-*Trans* (170.3)	s-*Trans* (−20.6)	1.59	4.9	s-*Trans* (167.4)	s-*Trans* (−4.2)	0.09	37.9
IV	s-*Cis* (19.2)	s-*Trans* (27.9)	2.05	2.2	s-*Cis* (−3.8)	s-*Trans* (4.3)	0.95	8.7
Experimental[B]	s-*Cis* (30.1)	s-*Cis* (−150.0)	5.84	–	s-*Cis* (−19.1)	s-*Trans* (22.5)	6.29	–
V[E]	s-*Cis* (−3.0)	s-*Cis* (161.8)	0.83	–	s-*Cis* (3.8)	s-*Trans* (−4.3)	0.95	–

[A]Calculated at the B3LYP/6–311G(d, p) level of theory.
[B]From X-ray diffraction data.
[C]ΔE_p ($= E_{p(i)} - E_{p(I)}$ kcal mol^{-1}) represents the potential energy difference between the conformer (i) and the most stable conformer (I).
[D]'Pop.' (in %) represents population based on energies and Maxwell–Boltzmann statistics.
[E]From X-ray diffraction data after optimization [B3LYP/6–311G(d,p)].

(torsion angle B in Chart 2). On the other hand, the ester carbonyl group is somewhat out of co-planarity with respect to the naphthyl residue as well. Here, also two orientations of C=O can be represented, that towards H8″ or s-*cis* configuration and that towards H2″ or s-*trans* configuration. All compounds of this series show the s-*cis* configuration, the torsion angles ψ(O3–C3–C1′–C9′) are between 1° and 44° for **1–6** but again larger for **7** (44°). Although the s-*cis* configuration is probable, it is poorly populated ($\Delta E_p > 1$ kcal mol^{-1}), as discussed above. In compound **7**, the change in the acetyl orientation, caused by steric interference with the *ortho*-methoxy group, affects the conformation of the remaining naphthoate as well. This is reasonable as O3 and H8′ are rather close to each other. Moreover, across this series, this relatively short intramolecular interatomic distance O3···H8 is in the range of 2.22–236 Å, but is somewhat longer for compound 7 (2.46 Å, Fig. 2 and Table 3).

*2-Naphthoates **8–13***

All conformational features of the naphthoates **8**–**13** are similar to those of **1**–**7**, except for the fact that the through-space interaction between the acetyl and the naphthoate residues noted for **1**–**7** does not exist in the 2-naphthoates **8**–**13**, at least not in the same magnitude (Fig. 3). There is no significant difference in the ψ(O3–C3–C2′–C1′) for **13** as compared with those of **8**–**12** (absolute ψ-values are between 6° and 22°). Looking at the conformations determined by the X-ray diffraction measurements, it becomes clear that in the 2-naphthoates, steric interaction across the molecule – as noted for the 1-naphthoates – is much less severe. All these compounds show the same naphthyl group disposition with respect to the carbonyl group (C1″ anti-periplanar to O3, s-*trans* configuration, Table 5), with the angle C3C2″C1″ (121–123°) greater than C3C2″C3″ (118°), except for compound **12** where C1″ approaches O3 (s-*cis* configuration, see Table 5). In this case, an opposite trend in the angles is observed (118° and 122°, respectively). Again, as stated above, the arrangement of the molecule of **12** in the crystal approaches the calculated highest energy conformer (Table 1), but it is only 0.95 kcal mol^{-1} higher than the most stable conformation. The observed contacts around the acetyl and ester oxygen atoms formed with different proton donor atoms for compounds **8**–**13** are listed in Table 6. From these results, it follows that the structure where the largest number of contacts on the ester group are established is precisely compound **12**; hence, this might explain their distinctive molecular conformations observed in the crystal. Fig. 4 shows contacts in the structures of **11** and **12**. This comparison is illustrative to show the effect of these interactions in stabilizing the carbonyl s-*cis* configuration of **12**. Note that such contacts are absent in the s-*trans* configuration of compound **11**.

Another way to investigate the effect of substituents on the structural parameters is by vibrational spectroscopy.[11] There is a direct correlation between the strength of the chemical bond (force constant) and the corresponding stretching frequencies.

Table 2. Crystal data of the new compounds 2–13[A]

	1-Naphthoates					
	2	**3**	**4**	**5**	**6**	**7[B]**
Formula	$C_{19}H_{13}NO_5$	$C_{19}H_{13}BrO_3$	$C_{19}H_{13}ClO_3$	$C_{19}H_{13}FO_3$	$C_{20}H_{16}O_3$	$C_{21}H_{18}O_5$
M_r	335.30	369.20	324.74	308.29	304.33	350.35
Crystal system	Monoclinic	Monoclinic	Monoclinic	Monoclinic	Monoclinic	Triclinic
Space group	$P2_1/c$	$P2_1/c$	$P2_1/c$	$P2_1/c$	$P2_1/c$	P
a [Å]	7.324(1)	7.459(1)	7.418(1)	12.341(2)	11.752(1)	7.500(1)
b [Å]	7.408(1)	7.394(1)	7.400(1)	10.767(2)	8.481(1)	9.251(1)
c [Å]	29.149(7)	28.624(2)	28.366(3)	12.797(2)	17.412(2)	12.705(2)
β [°]	95.46(2)	95.15(1)	95.58(2)	118.66(2)	114.20(1)	82.53(2)
V [Å^3]	1574.3(5)	1572.3(3)	1549.7(3)	1492.1(4)	1582.9(3)	861.7(2)
Z	4	4	4	4	4	2
D_c [g cm^{-1}]	1.415	1.560	1.392	1.372	1.277	1.350
Absorpt. coeff. [mm^{-1}]	0.104	2.627	0.259	0.101	0.085	0.096
F(000)	696	744	672	640	640	368
Crystal size [mm^3]	0.37 × 0.31 × 0.07	0.41 × 0.37 × 0.17	0.39 × 0.24 × 0.25	1.5 × 0.92 × 0.74	0.59 × 0.48 × 0.33	0.52 × 0.44 × 0.37
θ_{min}–θ_{max} [°]	2.79–20.21	2.74–24.12	2.76–20.94	2.62–24.12	1.90–24.14	2.23–24.17
hkl range	−7 to 7; −7 to 7; −28 to 29	−8 to 8; −8 to 8; −32 to 32	−7 to 7; −7 to 7; −26 to 28	−14 to 12; −12 to 12; −13 to 13	−13 to 13; −9 to 9; −19 to 19	−8 to 8; −10 to 10; −14 to 14
Reflections collected	5448	7786	5527	5035	11659	7083
Unique reflections	1673 (R_{int} = 0.1042)	2374 (R_{int} = 0.0504)	1647 (R_{int} = 0.0407)	2260 (R_{int} = 0.0663)	2479 (R_{int} = 0.0601)	2562 (R_{int} = 0.0542)
Unique reflections/ refinement parameters	13.07	11.36	7.88	10.76	11.75	10.76
R ($F2 > 2\sigma(F2)$)	0.207	0.041	0.030	0.046	0.036	0.039
wR ($F2$)	0496	0.099	0.043	0.098	0.075	0.091
S	1.15	1.13	0.86	1.22	1.14	1.21
$\Delta\rho_{max}$, $\Delta\rho_{min}$ [e Å^{-3}]	0.607, −0.458	0.406, −0.593	0.139, −0.130	0.168, −0.185	0.15, −0.136	0.15, −0.19
	2-Naphthoates					
	8	**9**	**10**	**11**	**12**	**13**
Formula	$C_{19}H_{13}NO_5$	$C_{19}H_{13}BrO_3$	$C_{19}H_{13}ClO_3$	$C_{19}H_{13}FO_3$	$C_{20}H_{16}O_3$	$C_{21}H_{18}O_5$
M_r	335.30	369.20	324.74	308.29	304.33	350.35
Crystal system	Orthorhombic	Orthorhombic	Monoclinic	Orthorhombic	Monoclinic	Monoclinic
Space group	$Pcab$	$Pcab$	$P2_1$	$F2dd$	$P2_1/c$	$P2_1/a$
a [Å]	8.252(1)	8.518(1)	4.905(1)	4.294(1)	10.209(1)	15.108(2)
b [Å]	11.454(2)	11.147(1)	11.537(1)	32.468(6)	10.541(1)	8.241(1)
c [Å]	33.739(3)	33.371(2)	13.917(2)	42.489(5)	15.586(2)	14.772(2)
β [°]	90	90	90.50(2)	90	110.37(1)	104.54(1)
V [Å^3]	3189.0(7)	3168.6(5)	787.5(2)	5924(2)	1572.4(3)	1780.3(4)
Z	8	8	2	16	4	4
D_c [g cm^{-1}]	1.397	1.548	1.369	1.383	1.286	1.307
Absorpt. coeff. [mm^{-1}]	0.10	2.607	0.254	0.10	0.086	0.09
F(000)	1392	1488	336	2560	640	736
Crystal size [mm^3]	5.5 × 0.10 × 0.08	2.2 × 0.07 × 0.06	0.7 × 0.21 × 0.16	1.9 × 0.11 × 0.03	0.52 × 0.33 × 0.26	0.41 × 0.28 × 0.20
θ_{min}–θ_{max} [°]	2.15–20.94	12.20–20.90	2.3–24.1	1.6–20.9	2.13–23.80	2.8–23.4
hkl range	−7 to 7; −11 to 11; −31 to 33	−8 to 8; −11 to 11; −29 to 33	−5 to 5; −13 to 13; −15 to 15	−4 to 4; −32 to 32; −40 to 42	−11 to 11; −12 to 12; −17 to 17	−17 to 17; −9 to 9 ; −16 to 16
Reflections collected	11581	10664	6448	6259	13345	13208
Unique reflections	1642 (R_{int} = 0.0636)	1621 (R_{int} = 0.0689)	2471 (R_{int} = 0.0384)	926 (R_{int} = 0.103)	2483 (R_{int} = 0.0613)	2801 (R_{int} = 0.0540)
Unique reflections/ refinement parameters	7.23	7.75	11.77	4.43	11.77	11.77
R ($F2 > 2\sigma(F2)$)	0.034	0.028	0.028	0.030	0.037	0.037
wR ($F2$)	0.048	0.037	0.042	0.050	0.074	0.051
S	0.96	0.94	0.98	0.78	1.07	1.07
$\Delta\rho_{max}$, $\Delta\rho_{min}$ [e Å^{-3}]	0.156, −0.174	0.226, −0.238	0.084, −0.151	0.09, −0.13	0.20, −0.175	0.13, −0.14

[A]MoKα radiation, λ = 0.71073 Å.

[B]α (°): 89.88(2); β (°): 82.53(2); γ (°): 80.43(2).

Table 3. Selected interatomic distances (*d*) (in Å) and infrared carbonyl ($\nu_{C=O}$) stretching frequencies of 1–13 (in cm^{-1})

1-Naphthoates	C1–O1	$\nu_{C=O}$	C1–C1′	C1′–C2′	C2′–O2	O2–C3	C3–O3	$\nu_{C=O}$	C3–C1″	O3···H8″	O2···H8″	O1–O3
1 (H)	1.210(2)	1685	1.499(2)	1.394(2)	1.404(1)	1.360(2)	1.195(2)	1726	1.491(2)	2.22	4.02	3.20
2 (NO_2)	1.16(2)	1686	1.52(2)	1.35(2)	1.42(2)	1.37(2)	1.25(2)	1742	1.43(2)	2.29	3.93	5.35
3 (Br)	1.206(4)	1683	1.504(5)	1.382(4)	1.402(4)	1.363(4)	1.201(4)	1732	1.469(4)	2.32	3.94	5.38
4 (Cl)	1.214(3)	1683	1.493(4)	1.385(3)	1.403(3)	1.372(3)	1.195(3)	1734	1.485(3)	2.32	3.94	5.35
5 (F)	1.214(3)	1680	1.496(4)	1.390(3)	1.385(3)	1.394(3)	1.197(3)	1732	1.458(3)	2.22	4.08	3.04
6 (CH_3)	1.215(2)	1680	1.500(2)	1.383(2)	1.400(2)	1.3494(19)	1.203(2)	1732	1.486(2)	2.36	3.93	3.28
7 (bis-CH_3O)	1.217(2)	1663	1.477(3)	1.394(2)	1.405(2)	1.364(2)	1.206(2)	1738	1.467(3)	2.46	3.78	3.03

2-Naphthoates	C1–O1	$\nu_{C=O}$	C1–C1′	C1′–C2′	C2′–O2	O2–C3	C3–O3	$\nu_{C=O}$	C3–C2″	O1–O3
8 (NO_2)	1.207(4)	1696	1.517(4)	1.373(4)	1.404(3)	1.365(4)	1.195(4)	1740	1.490(4)	3.62
9 (Br)	1.205(5)	1690	1.500(5)	1.374(5)	1.403(4)	1.366(5)	1.201(5)	1738	1.475(5)	3.44
10 (Cl)	1.205(3)	1690	1.487(4)	1.374(4)	1.390(3)	1.366(4)	1.192(4)	1738	1.469(4)	3.29
11 (F)	1.216(5)	1696	1.482(6)	1.403(6)	1.396(5)	1.365(5)	1.206(6)	1724	1.460(6)	3.75
12 (CH_3)	1.202(2)	1680	1.492(3)	1.399(3)	1.406(2)	1.361(2)	1.204(2)	1728	1.473(3)	3.15
13 (bis-CH_3O)	1.221(2)	1668	1.480(3)	1.400(3)	1.406(2)	1.365(2)	1.210(2)	1731	1.476(3)	3.24

Table 4. Selected interatomic angles of 1–14 (in degrees)

R (*1-Naphthoates*)	O1C1C2	C1′C1C2	C1′C1O1	C2′C1′C1	C1′C2′O2	C3′C2′O2	C2′O2C3	O2C3C1″	O3C3C1″	C3C1″C2″	C3C1″C9″
1 (H)	120.37(17)	118.65(16)	120.98(16)	122.29(12)	120.00(12)	117.87(15)	117.54(11)	110.94(12)	127.36(16)	118.82(13)	121.04(12)
2 (NO_2)	119.4(19)	117.9 (18)	122.7(17)	129.3(16)	118.4(15)	116.1(15)	119.8(12)	114.3(14)	125.8(15)	116.3(14)	124.7(14)
3 (Br)	119.3(3)	121.4(3)	119.3(3)	125.5(3)	119.4(3)	117.5(3)	119.0(2)	110.6(3)	127.8(3)	118.3(3)	121.7(3)
4 (Cl)	119.8(3)	121.1(3)	119.2(3)	126.4(3)	119.1(3)	117.4(3)	118.1(2)	109.5(2)	128.1(3)	118.7(3)	121.0(2)
5 (F)	119.1(3)	118.8(2)	122.1(2)	121.8(2)	122.5(2)	115.9(2)	116.57(18)	111.3(2)	129.5(2)	119.9(2)	120.8(2)
6 (CH_3)	121.08(18)	119.16(19)	119.74(17)	121.98(17)	119.42(15)	118.16(17)	119.51(14)	110.09(16)	127.21(17)	118.58(16)	121.41(17)
7 (bis-CH_3O)	117.94(18)	120.78(17)	121.23(16)	121.32(17)	119.30(16)	116.20(16)	118.27(14)	110.38(16)	127.49(16)	119.15(18)	120.71(17)

R (*2-Naphthoates*)	O1C1C2	C1′C1C2	C1′C1O1	C2′C1′C1	C1′C2′O2	C3′C2′O2	C2′O2C3	O2C3C2″	O3C3C2″	C3C2″C1″	C3C2″C3″
8 (NO_2)	122.8(3)	117.6(3)	119.6(4)	121.9(3)	118.9(3)	117.8(3)	117.7(3)	111.4(3)	125.9(4)	120.9(3)	118.4(3)
9 (Br)	121.2(4)	117.2(4)	121.5(4)	121.6(4)	119.6(3)	117.4(4)	117.3(3)	111.7(4)	126.3(5)	121.8(4)	117.8(4)
10 (Cl)	118.5(3)	119.8(3)	121.7(3)	123.5(3)	121.4(3)	116.0(3)	117.9(2)	112.1(3)	126.7(3)	121.6(3)	118.1(3)
11 (F)	118.0(5)	118.8(5)	123.2(5)	122.2(5)	119.0(5)	119.1(6)	117.8(4)	112.4(5)	126.8(6)	122.8(5)	117.8(5)
12 (CH_3)	118.9(2)	120.2(2)	120.8(2)	123.07(18)	122.06(18)	115.87(18)	117.92(16)	112.1(2)	125.9(2)	117.9(2)	122.4(2)
13 (bis-CH_3O)	118.9(2)	120.8(2)	120.2(2)	121.3(2)	117.0(2)	118.6(2)	118.73(18)	111.6(2)	126.1(2)	121.6(2)	118.5(2)

The intense stretching carbonyl band in infrared spectroscopy is particularly valuable to monitor the strength of the chemical bond.

It is well known that C=O stretching frequencies of esters (–C(=O)–O–R) are higher than ketones due to their electron acceptor oxygen atom (–O–R). This inductive effect that reinforces the force constant (and the bond order) is more important than the weakening produced by resonance with the electron pair on the oxygen (–C(–O$^-$)=O$^+$–R).[11]

The values found for the ν_{CO} frequencies of the acetyl group are between 1680 and 1696 cm^{-1} for all naphthoyl esters except for compounds **7** and **13**, wherein respective values of 1663 and 1668 cm^{-1} are observed. This shifting to lower frequencies, observed in the latter two compounds, is consistent with a weakening of the C=O bond caused by steric interference of the methoxy group at position 6 ($d_{C1O1} = 1.217$ and 1.221 Å for **7** and **13**, respectively; d = interactomic distance). Finally, as above stated, d_{C3O3} values are shorter than d_{C1O1} values for all compounds studied because the force constant of the C=O bond in the ester moiety is enhanced by the electron-withdrawing nature of the adjacent oxygen atom.[11] As expected, the frequency of the ester carbonyl stretching is shifted to higher values (1724–1742 cm^{-1}).

With help of computational analysis, it is clear that the 1-naphthotate series has a distinctive behaviour: the carbonyl of acetyl and ester functions ($ArCOCH_3$/ArOCONaph) concentrates up to 92–94 % of the population in gas phase in the two most stable conformations (s-*trans*/s-*cis* and s-*cis*/s-*cis*). In these two conformations, the naphthoyl has a s-*cis* configuration. This finding is in agreement with the X-ray diffraction results for the 1-naphthoyl series, **1**–**7**, as they all have this conformation. In **4**, the most stable calculated molecular conformation in the gas phase agrees with that obtained from X-ray diffraction data. Compounds **1** and **6** have an arrangement similar to the second most stable predicted conformation ($\Delta E_p < 1$ kcal mol^{-1}). Although the fluorine derivative (compound **5**) was not analyzed by theoretical calculations, comparable results should be expected. The intermolecular interaction seems to be responsible for this particular preference in the

Table 5. Selected experimental torsion angles of 1–13 (in degrees)

	Space group	δ^A	φ^B	φ^C	ψ^D	Conf. C=O[E]	
						Acetyl	Ester
				1-Naphthoates			
1 (H)	$P2_1/n$	−77	63.1(2)	−24.2(2)	65.3(2)	s-*Cis*	s-*Cis*
2 (NO$_2$)	$P2_1/c$	68.8(5)	−57(2)	−154(2)	68(2)	s-*Trans*	s-*Cis*
3 (Br)	$P2_1/c$	69.8(1)	−66.1(4)	−159.9(3)	64.8(5)	s-*Trans*	s-*Cis*
4 (Cl)	$P2_1/c$	67.49(6)	−64.4(4)	−159.5(3)	64.9(4)	s-*Trans*	s-*Cis*
5 (F)	$P2_1/c$	60.86(6)	−72.0(3)	64.2(4)	6.8(4)	s-*Cis*	s-*Cis*
6 (CH$_3$)	$P2_1/c$	68.00(4)	−50.6(2)	60.1(3)	60.5(3)	s-*Cis*	s-*Cis*
7 (bis-CH$_3$O)	*P*-1	−41.80(6)	−23.5(3)	62.9(4)	64.2(3)	s-*Cis*	s-*Cis*
				2-Naphthoates			
8 (NO$_2$)	*Pcab*	66.04(7)	−62.8(3)	−31.3(5)	−165.2(4)	s-*Cis*	s-*Trans*
9 (Br)	*Pcab*	69.93(9)	−67.2(4)	−30.6(7)	−161.1(5)	s-*Cis*	s-*Trans*
10 (Cl)	$P2_1$	66.57(9)	−91.8(4)	6.3(8)	−171.2(5)	s-*Cis*	s-*Trans*
11 (F)	*F2dd*	66.2(1)	−72.3(6)	−15(1)	−173.5(6)	s-*Cis*	s-*Trans*
12 (CH$_3$)	$P2_1/c$	62.00(7)	−28.0(3)	−19.1(3)	62.5(4)	s-*Cis*	s-*Cis*
13 (bis-CH$_3$O)	$P2_1/a$	63.84(4)	−77.2(2)	−41.0(3)	−174.0(2)	s-*Cis*	s-*Trans*

[A]δ: diedral angle between ring planes.
[B]φ: ∠(C1′C2′C1″C9″) in 1-naphthyl derivatives. φ: ∠(C1′C2′C2″C1″) in 2-naphthyl derivatives.
[C]φ: ∠(O1C1C1′C2′).
[D]ψ: ∠(O3C3C1″C9″) in 1-naphthyl derivatives. ψ: ∠(O3C3C2″C1″) in 2-naphthyl derivatives.
[E]Configuration: acetyl: Ar–C(=O)–CH_3; ester: Ar–O–C(=O)–naph.

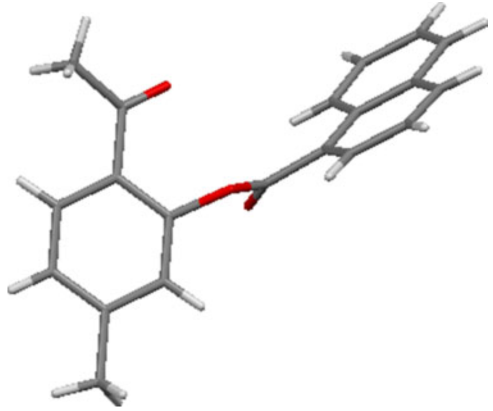

Fig. 1. Capped-sticks plot of **6**. The ring atoms C1′–C6′ are in the drawing plane.

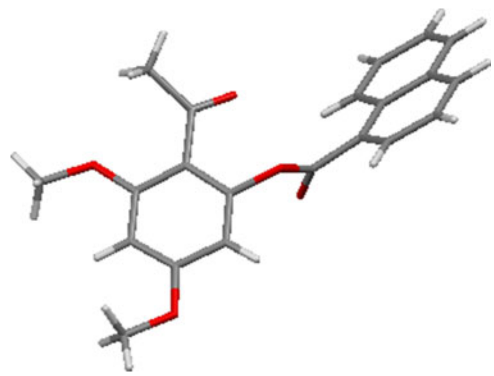

Fig. 2. Capped-sticks plot of **7**. The ring atoms C1′–C6′ are in the drawing plane.

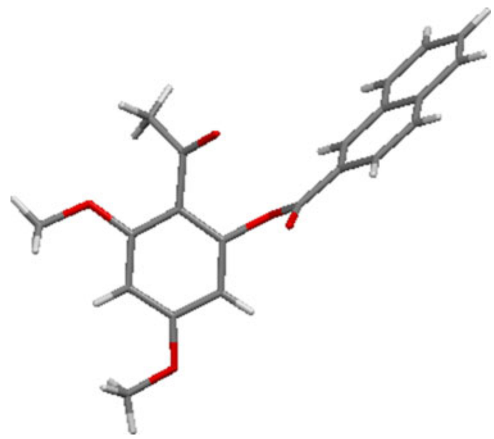

Fig. 3. Capped-sticks plot of **13**. The ring atoms C1′–C6′ are in the drawing plane.

crystal packing. In addition, around the acetyl and ester oxygen atoms of compounds **1**–**7**, short contacts are formed with different proton donor atoms, but the results are not as conclusive as those observed for the 2-naphthoyl series.

Infrared spectroscopy was used as a second spectroscopic tool to monitor some structural parameters in solid state. The carbonyl stretching frequency $\nu_{C=O}$ was valuable to confirm the weakening of the chemical bond as a consequence of steric interference in the 2,6-dimetoxy-substituted compounds **7** and **13**.

Conclusion

Phenyl aroates are well-known aromatic molecules containing two planes connected by the ester functionality (–C(=O)–O–), which gives some flexibility to the molecular structure. Theoretical calculations were useful for evaluating the stability of different conformations and determining which of the possible

Table 6. Observed contacts formed by the acetyl and ester oxygen atoms: bond length (in Å) and bond angle (in degrees)[A]

8	**D···A**	**H···A**	**D–H···A**	**11**	**D···A**	**H···A**	**D–H···A**
C1′–H1′···O2	2.710(4)	2.377(2)	100.8(2)	C1′–H7···O2	2.721(7)	2.387(4)	101.0(4)
C3′–H3′···O3	2.882(4)	2.620(2)	96.7(2)	C3′–H8···O3	2.864(7)	2.597(4)	97.1(3)
C1′–H1′···O1$^{(i)}$	3.621(4)	2.757(3)	154.9(2)	C2–H3···O3$^{(viii)}$	3.471(7)	2.563(4)	157.7(4)
C2–H2C···O3$^{(i)}$	3.541(5)	2.656(3)	153.5(2)	C1′–H7···O1$^{(ix)}$	3.376(7)	2.513(4)	154.6(3)
C5′–H5′···O3$^{(ii)}$	3.353(4)	2.464(2)	160.0(2)				
C6′–H6′···O1$^{(iii)}$	3.598(4)	2.973(2)	125.8(2)				
9				**12**			
C1′–H7···O2	2.729(4)	2.404(2)	100.3(2)	C3′–H11···O2	2.776(3)	2.494(2)	97.7(1)
C3′–H8···O3	2.877(5)	2.623(3)	96.3(3)	C1′–H10···O3	2.858(3)	2.580(2)	97.8(1)
C1′–H7···O1$^{(i)}$	3.588(5)	2.716(4)	156.5(2)	C4–H6···O1$^{(x)}$	3.655(4)	2.819(2)	146.0(2)
C2–H3···O3$^{(i)}$	3.487(6)	2.619(3)	150.5(3)	C5′–H8···O1$^{(x)}$	3.484(3)	2.735(2)	138.3(1)
C5′–H5···O3$^{(ii)}$	3.387(5)	2.482(3)	164.4(3)	C6′–H9···O3$^{(xi)}$	3.550(3)	2.643(2)	165.4(1)
C6′–H11···O1$^{(iv)}$	3.762(5)	2.991(3)	141.3(3)	C1′–H10···O3$^{(xii)}$	3.520(2)	2.681(1)	150.5(1)
				C8′–H16···O3$^{(xii)}$	3.554(3)	2.721(2)	149.4(2)
				C6′–H14···O1$^{(xiii)}$	3.509(4)	2.903(2)	124.0(2)
				C5′–H13···O1$^{(xiii)}$	3.465(4)	2.811(3)	128.3(2)
10				**13**			
C1′–H7···O2	2.705(4)	2.370(2)	100.9(3)	C1′–H12···O2	2.702(3)	2.359(2)	101.4(1)
C3′–H8···O3	2.860(6)	2.598(3)	96.7(3)	C3′–H13···O3	2.872(3)	2.599(2)	97.4(2)
C6′–H6···O3$^{(v)}$	3.155(6)	2.362(3)	143.1(3)	C7′–H7···O3$^{(xiv)}$	3.520(3)	2.564(1)	174.2(1)
C1′–H7···O1$^{(vi)}$	3.503(6)	2.650(4)	152.9(3)	C7′–H8···O1$^{(xv)}$	3.452(3)	2.843(2)	122.3(1)
C5′–H10···O1$^{(vii)}$	3.602(7)	2.940(3)	129.3(4)	C7′–H8···O3$^{(xv)}$	3.509(3)	2.653(2)	148.7(1)
				C8′–H9···O1$^{(xvi)}$	3.838(3)	2.912(2)	162.6(1)
				C6′–H16···O1$^{(xvii)}$	3.453(4)	2.730(2)	135.3(2)

[A]Symmetry codes: (i) $x - 1/2, -y + 1/2, z$; (ii) $-x + 1/2, y + 1/2, -z + 1$; (iii) $x, y - 1/2, -z + 1/2$; (iv) $x - 1/2, -y, -z + 1/2$; (v) $-x + 2, y + 1/2, -z + 1$; (vi) $x - 1, y, z$; (vii) $-x + 1, y - 1/2, -z$; (viii) $x - 1/4, y + 1/4, -z + 3/4$; (ix) $x - 1, y, z$; (x) $x, -y + 1/2, z + 1/2$; (xi) $-x, y + 1/2, -z + 1/2$; (xii) $-x, -y, -z$; (xiii) $-x + 1, -y, -z$; (xiv) $x - 1/2, -y + 1/2, z$; (xv) $-x, -y + 1, -z + 1$; (xvi) $x - 1/2, -y + 3/2, z$; (xvii) $-x + 1/2, y - 1/2, -z$.

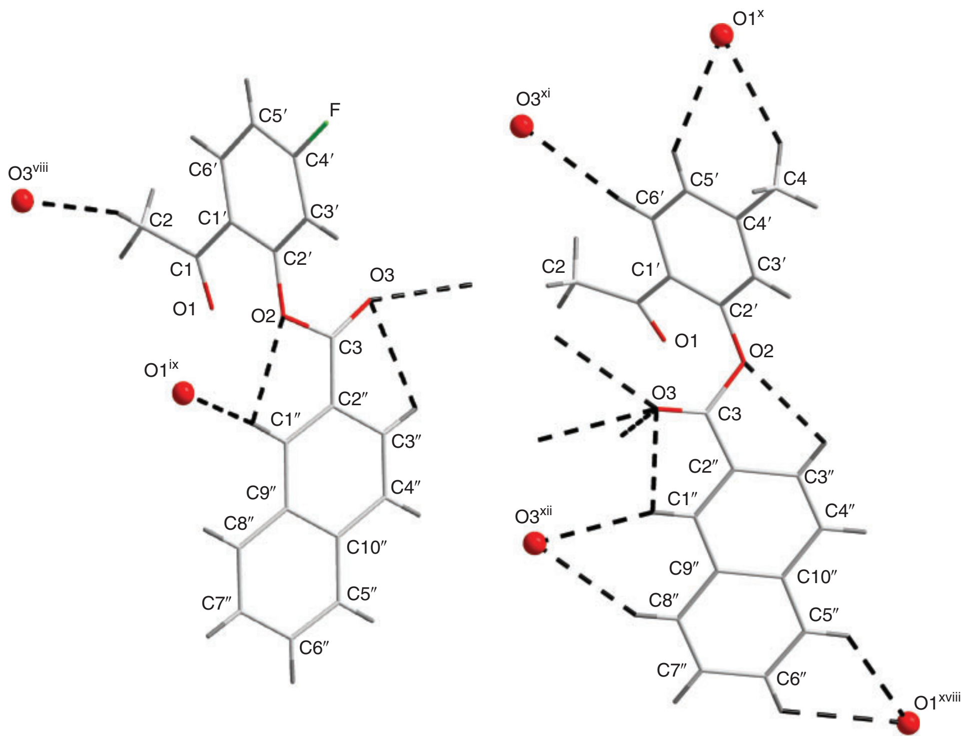

Fig. 4. Wireframe representations of (a) **11** and (b) **12** showing contacts formed by the acetyl and ester oxygen atoms. Oxygen atom notations as explained in Table 6.

conformations was significantly populated and therefore could exist in the crystal. The data obtained by X-ray diffraction were valuable to show the relative spatial orientation between planes. The distinctive configuration adopted for **12** in the crystal could be explained in terms of the higher number of contacts around the oxygen atom in the ester function.

Infrared spectroscopy was used as a second spectroscopic tool to monitor some structural parameters in solid state. The carbonyl stretching frequency $\nu_{C=O}$ was valuable to confirm the weakening of the chemical bond as a consequence of steric interference in the 2,6-dimetoxy-substituted compounds **7** and **13**. The inverse relationship between bond length and stretching frequency C=O was noted throughout the studied series.

Experimental

The preparation procedures of compounds **2**–**13**,[12] melting points, yields, and results of elemental analysis have been reported previously (Chart 2).[9,13] The X-ray data of **1** were published previously.[7] The infrared spectra were recorded in KBr pellets in the range of 4000–400 cm^{-1} on a Thermo Scientific Nicolet IR200 Fourier transform infrared spectrometer (2 cm^{-1} resolution).

Computational Details

The density functional theory[14–16] was used to perform the conformational analysis of **1** and its constitutional isomer (*o*-acetylphenyl 2-naphthoate) in order to determine its more stable conformers. The calculations were accomplished using Becke's three-parameters hybrid density functional[17] with the gradient-corrected correlation functional according to Lee, Yang, and Parr,[18] a combination that gives rise to the well-known B3LYP method. Potential energy curves of **1** were obtained by performing a relaxed scan around ψ(O1C1–C1′C2′) torsion angle A, ψ(C1′C2′–O2C3) torsion angle B, ψ(C2′O2–C3O3) torsion angle C, and ψ(O3C3–C1″C2″) (or O3C3–C2″C1″) torsion angle D, at a B3LYP/6–31 g(d) level of theory, see Chart 2 for labels (capital letters for torsion angles and bonds in blue colour).

The geometry of those conformers that became a minimum on the potential energy curves mentioned in the previous paragraph was further optimized at a B3LYP/6–311 g(d,p) level of theory. The Hessian matrix of the energy with respect to the nuclear coordinates was constructed and diagonalized for the most stable conformers to confirm whether they are true minima or saddle points on the potential energy surface of the molecule. The eigenvalues of the Hessian matrix of the stable conformers were further used in a statistical analysis to obtain total energies. All calculations were carried out with the *Gaussian 03* package.[19]

X-Ray Crystallography

Suitable crystals were obtained by slow evaporation from saturated solutions of acetonitrile (**2**, **4–7**, **9**, and **11**) or methanol (**3**, **8**, **10**, **12**, and **13**). Single-crystal X-ray diffraction experiments were carried out with a Stoe IPDS (area detector) diffractometer using graphite monochromated MoKα radiation at room temperature. The data collection in each case covered almost a full sphere of reciprocal space within $2\theta_{max}$ of ~42–48°. Due to the fact that each crystal was rotated only about one axis, the reflections of a small part of the reciprocal lattice were not accessible. A second measurement using another rotation axis was thought to be unnecessary. A few reflections with very low 2θ (<3.6°) could not be measured due to collision with the primary beam stop. In some cases, the strongest reflections exceeded the intensity range of the imaging plate. The repetition of the measurement using a shorter exposure time, likewise, was thought to be unnecessary. The completeness of the unique dataset was ~93 % for the triclinic crystal (compound **7**) and 95–100 % for the monoclinic and orthorhombic ones (compounds **2–6**, **8–13**). The completeness of the datasets was sufficient in all cases to solve the structures using *SHELXS*.[20] The number of measured reflections exceeded the number of unique reflections by factors in the range of 2.3–7.7 depending on symmetry. Intensity integration and data reduction were performed using the *Stoe IPDS* software.[21] The structures were solved by direct methods (*SHELXS*)[20] and refined by full matrix least-squares against F^2 of all data (*SHELXL*).[22] The ratio of the number of unique reflections to the number of refined parameters varied from 4.43 to 13.07.

Non-hydrogen atoms were refined using anisotropic displacement parameters with one exception concerning compound **2**. The low quality of the reflection dataset and final *R*-values of compound **2** resulted from a twin problem which could not be resolved satisfactorily. Hydrogen atom positions were calculated geometrically and included in the refinement as riding on the corresponding bound atom. Details of the individual measurements, data reductions, and structure refinements are reported in the CIFs. The most important crystallographic data and refinement parameters of compounds **2–13** are listed in Table 2, whereas selected interatomic distances, bond angles, and torsion angles in **1**–**13** are presented in Tables 3–5.

The program *PLATON*[23] was used for checks, and Figs 1–4 were created with *Mercury*.[24] Full crystallographic data (without structure factors) were deposited using the CIF format at the Cambridge Crystallographic Data Centre (12 Union Road, Cambridge CB2 1EZ, UK; fax: +44−1223/336−033; email: deposit@ccdc.cam.ac.uk) and can be obtained free of charge at www.ccdc.cam.ac.uk/conts/retrieving.html: CCDC no. 1030763 for **6**, CCDC no. 1030764 for **5**, CCDC no. 1030765 for **2**, CCDC no. 1030766 for **13**, CCDC no. 1030767 for **11**, CCDC no. 1030768 for **8**, CCDC no. 1030769 for **12**, CCDC no. 1030770 for **4**, CCDC no. 1030771 for **10**, CCDC no. 1030772 for **9**, CCDC no. 1030773 for **7**, and CCDC no. 1030774 for **3**.

Acknowledgements

J. J. thanks the German Academic Exchange Service (DAAD) for a fellowship at Hannover University.

References

[1] G. P. Ellis, in *Chemistry of Heterocyclic Compounds* (Ed. G. P. Ellis) **2008**, Vol. 31, pp. 455–480 (John Wiley & Sons, Inc.: Hoboken, NJ).

[2] A. K. Tewari, P. Srivastava, V. P. Singh, C. Puerta, P. Valerga, *ARKIVOC* **2010**, *2010*(*ix*), 127. doi:10.3998/ARK.5550190.0011.911

[3] D. M. Pawar, A. A. Khalil, D. R. Hooks, K. Collins, T. Elliott, J. Stafford, L. Smith, E. A. Noe, *J. Am. Chem. Soc.* **1998**, *120*, 2108. doi:10.1021/JA9723848

[4] J.-H. Lii, *J. Phys. Chem. A* **2002**, *106*, 8667. doi:10.1021/JP0142029

[5] K. B. Wiberg, K. E. Laidig, *J. Am. Chem. Soc.* **1987**, *109*, 5935. doi:10.1021/JA00254A006

[6] K. Byun, Y. Mo, J. Gao, *J. Am. Chem. Soc.* **2001**, *123*, 3974. doi:10.1021/JA001369R

[7] A. E. Goeta, G. Punte, J. L. Jios, J. C. Autino, *Acta Crystallogr., Sect. C: Cryst. Struct. Commun.* **1996**, *52*, 2045. doi:10.1107/S0108270196001266

[8] C. Kazak, M. Aygun, C. Kus, S. Ozbey, O. Buyukgungor, *Acta Crystallogr., Sect. E: Struct. Rep. Online* **2002**, *58*, o612. doi:10.1107/S1600536802007651

[9] J. L. Jios, H. Duddeck, *Z. Naturforsch.* **2000**, *55b*, 189.

[10] N. N. Buceta, D. Ruiz, G. P. Romanelli, J. C. Autino, H. Duddeck, R. Pis Diez, J. L. Jios, *J. Phys. Org. Chem.* **2014**, *27*, 106. doi:10.1002/POC.3246

[11] R. M. Silverstein, F. X. Webster, *Spectrometric Identification of Organic Compounds* **1998** (John Wiley & Sons, Inc.: New York, NY).

[12] J. L. Jios, J. C. Autino, A. B. Pomilio, *An. Asoc. Quím. Argent.* **1995**, *83*, 183.

[13] J. L. Jios, *Naftilcromonas, sulfonilbis(naftilcromonas) y compuestos relacionados* **1996**, Ph.D. thesis, La Plata University, Argentina.

[14] P. Hohenberg, W. Kohn, *Phys. Rev. B* **1964**, *136*, B864. doi:10.1103/PHYSREV.136.B864

[15] W. Kohn, L. J. Sham, *Phys. Rev. A* **1965**, *140*, A1133. doi:10.1103/PHYSREV.140.A1133

[16] R. G. Parr, W. Yang, *Density Functional Theory of Atoms and Molecules* **1989** (Oxford University Press: New York, NY).

[17] A. D. Becke, *J. Chem. Phys.* **1993**, *98*, 5648. doi:10.1063/1.464913

[18] C. Lee, W. Yang, R. G. Parr, *Phys. Rev. B* **1988**, *37*, 785. doi:10.1103/PHYSREVB.37.785

[19] M. J. Frisch, G. W. Trucks, H. B. Schlegel, G. E. Scuseria, M. A. Robb, J. R. Cheeseman, J. A. Montgomery Jr, T. Vreven, K. N. Kudin, J. C. Burant, J. M. Millam, S. S. Iyengar, J. Tomasi, V. Barone, B. Mennucci, M. Cossi, G. Scalmani, N. Rega, G. A. Petersson, H. Nakatsuji, M. Hada, M. Ehara, K. Toyota, R. Fukuda, J. Hasegawa, M. Ishida, T. Nakajima, Y. Honda, O. Kitao, H. Nakai, M. Klene, X. Li, J. E. Knox, H. P. Hratchian, J. B. Cross, V. Bakken, C. Adamo, J. Jaramillo, R. Gomperts, R. E. Stratmann, O. Yazyev, A. J. Austin, R. Cammi, C. Pomelli, J. W. Ochterski, P. Y. Ayala, K. Morokuma, G. A. Voth, P. Salvador, J. J. Dannenberg, V. G. Zakrzewski, S. Dapprich, A. D. Daniels, M. C. Strain, O. Farkas, D. K. Malick, A. D. Rabuck, K. Raghavachari, J. B. Foresman, J. V. Ortiz, Q. Cui, A. G. Baboul, S. Clifford, J. Cioslowski, B. B. Stefanov, G. Liu, A. Liashenko, P. Piskorz, I. Komaromi, R. L. Martin, D. J. Fox, T. Keith, M. A. Al-Laham, C. Y. Peng, A. Nanayakkara, M. Challacombe, P. M. W. Gill, B. Johnson, W. Chen, M. W. Wong, C. Gonzalez, J. A. Pople, *Gaussian 03 Revision B.04* **2003** (Gaussian, Inc.: Wallingford, CT).

[20] G. M. Sheldrick, *SHELXS-86. Program for Crystal Structure Determination* **1986** (University of Göttingen: Göttingen).

[21] *STOE-IPDS Software Package: Programs for Data Collection with the IPDS Diffractometer and Data Reduction* **1995** (Stoe: Darmstadt).

[22] G. M. Sheldrick, *SHELXL-97. A Program for Refining Crystal Structures* **1997** (University of Göttingen: Göttingen).

[23] A. Spek, *Acta Crystallogr., Sect. A: Found. Crystallogr.* **1990**, *46*, c34.

[24] C. F. Macrae, P. R. Edgington, P. McCabe, E. Pidcock, G. P. Shields, R. Taylor, M. Towler, J. van de Streek, *J. Appl. Cryst.* **2006**, *39*, 453. doi:10.1107/S002188980600731